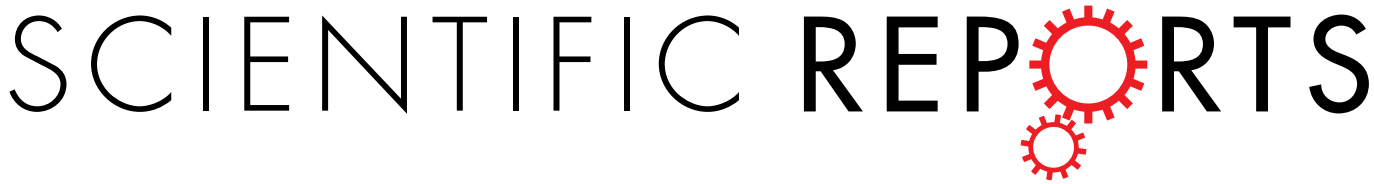

OPEN

Thermal catalytic oxidation of octachloronaphthalene over anatase TiO_2 nanomaterial and its hypothesized mechanism

Received: 09 September 2015
Accepted: 06 November 2015
Published: 08 December 2015

Guijin Su, Qianqian Li, Huijie Lu, Lixia Zhang, Linyan Huang, Li Yan & Minghui Zheng

As an environmentally-green technology, thermal catalytic oxidation of octachloronaphthalene (CN-75) over anatase TiO_2 nanomaterials was investigated at 300 °C. A wide range of oxidation intermediates, which were investigated using various techniques, could be of three types: naphthalene-ring, single-benzene-ring, and completely ring-opened products. Reactive oxygen species on anatase TiO_2 surface, such as $O_2^{-\bullet}$ and O^{2-}, contributed to oxidative degradation. Based on these findings, a novel oxidation degradation mechanism was proposed. The reaction at (101) surface of anatase TiO_2 was used as a model. The naphthalene-ring oxidative products with chloronaphthols and hydroxyl-pentachloronaphthalene-dione, could be formed via attacking the carbon of naphthalene ring at one or more positions by nucleophilic O^{2-}. Lateral cleavage of the naphthalene ring at different C_1-C_{10} and C_4-C_9, C_1-C_2 and C_4-C_9, C_1-C_2 or and C_3-C_4 bond positions by electrophilic $O_2^{-\bullet}$ could occur. This will lead to the formation of tetrachlorophenol, tetrachloro-benzoic acid, tetrachloro-phthalaldehyde, and tetrachloro-acrolein-benzoic acid, partially with further transformation into tetrachlorobenzene-dihydrodiol and tetrachloro-salicylic acid. Unexpectedly, the symmetric half section of CN-75 could be completely remained with generating the intricate oxidative intermediates characteristically containing tetrachlorobenzene structure. Complete cleavage of naphthalene ring could produce the ring-opened products, such as formic and acetic acids.

As a new type of persistent organic pollutants, polychlorinated naphthalenes (PCNs) was proposed into Annexes A and C of the Stockholm Convention (SC) on POPs in 2015[1]. There are 75 possible PCN congeners, in eight homolog groups, with one to eight chlorine atoms substituted around the planar aromatic naphthalene molecule. PCNs have been widely used in many commercial products, e.g., for wood preservation, as additives to paints and engine oils, for cable insulation, and in capacitors. Because of the structural similarities between PCNs and polychlorinated biphenyls (PCBs), PCNs are present in technical PCB formulations[2,3]. Yamashita *et al.*[4] examined the concentrations and profiles of tri- through octa-chloro-substituted congeners in 18 technical PCB mixtures, and detected concentrations ranging from 5.2 to 730 μg/g. PCNs are also unintentionally generated during high-temperature industrial processes in the presence of chlorine. Of the known releases, waste incineration is considered to be the significant current source[5], with similar formation mechanism to that of polychlorinated dibenzo-p-dioxins and dibenzofurans (PCDD/Fs)[6]. The production and use of PCNs were banned in the United States and Europe in the 1980 s, because of their toxicity and environmental persistence[7]. Nevertheless, PCNs can be released from past use, products that have not yet been disposed of, devices containing PCBs still in use, and thermal processes such as waste incineration. In accordance with the relevant SC regulations,

State Key Laboratory of Environmental Chemistry and Ecotoxicology, Research Center for Eco-Environmental Sciences, Chinese Academy of Sciences, P.O. Box 2871, Beijing 100085, China. Correspondence and requests for materials should be addressed to G.S. (email: gjsu@rcees.ac.cn)

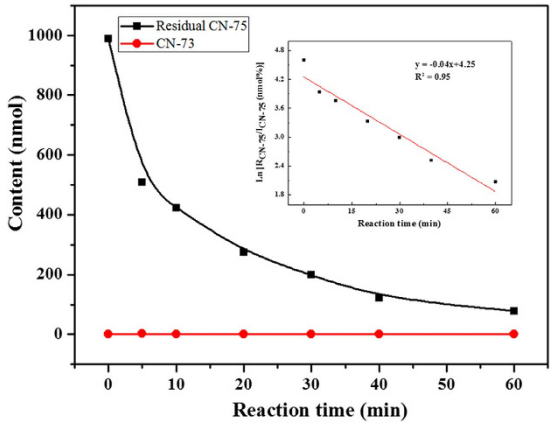

Figure 1. Contents of residual CN-75 and generated CN-73 as function of heating time. Inset shows pseudo-first-order kinetic plot of the reaction.

based on a risk management evaluation and consideration of the management options, the Committee recommended a Conference of the Parties to consider listing and specifying the relevant control measures for PCNs[8]. The reduction of PCN levels is therefore a matter of public concern in the context of environmental protection.

Catalytic oxidation for the removal of chlorinated aromatic hydrocarbons has attracted much attention as a green technique[9,10]. TiO_2-based catalysts are generally used for the oxidation of chlorinated aromatic compounds[11–14]. Lichtenberger *et al.*[12] examined the oxidation of chlorobenzene, and 1,2-, 1,3-, and 1,4-dichlorobenzene over V_2O_5/TiO_2 catalysts. A common reaction mechanism was proposed based on kinetic and *in situ* fourier transform infrared (FTIR) results. Surface phenolates are formed via nucleophilic attack at the chlorine position in the aromatic ring, followed by electrophilic substitution of the adsorbed partially dechlorinated species in the second step. Krishnamoorthy *et al.*[11] investigated the catalytic oxidations of 1,2-dichlorobenzene over Cr_2O_3, V_2O_5, MoO_3, Fe_2O_3, and Co_3O_4 supported on TiO_2 and Al_2O_3. The TiO_2-supported systems were more active than the corresponding Al_2O_3-supported ones, indicating that the support is significant in the catalytic performance of the catalyst in this reaction. Gannoun *et al.*[15] showed that sulfated TiO_2 nanotubes (HNTs) were a promising support for V_2O_5-based materials in the oxidative elimination of chlorobenzene. The formed bridged bidentate Ti and acidic sites on the HNT surface probably govern chlorobenzene oxidation and decrease the reducibility of vanadium, leading to higher reactivity at redox sites and therefore to higher-efficiency catalysts. Thus far, however, the reports to deeply identify the oxidation products and the associated mechanisms of PCNs as new POPs, are particularly scarce.

TiO_2 is an important semiconductor material and has been used in a variety of applications such as photosplitting of water[16], photovoltaic devices[17], liquid solar cells, surface wettability conversion, and degradation of toxic pollutants[18]. This wide range of applications can be attributed to its nontoxicity, low cost, photostability, redox efficiency, and availability. TiO_2 has three crystal form, i.e., brookite, anatase, and rutile. The crystal form of TiO_2 has a decisive effect on its catalytic performance, because the electronic band gaps (EBGs) of the different forms of TiO_2 are different. It has been reported that the photocatalytic activity of anatase TiO_2 is limited by its small absorption range in the solar spectrum, as a result of its large EBG ($Eg = 3.2$ eV). However, the larger EBG of anatase TiO_2 has attracted great interest in its better oxidation performance. Therefore, it is of significance that the catalytic oxidation of PCNs is performed by anatase TiO_2 with illustrating the involved deep oxidation mechanism.

In this study, the reactivity of an anatase TiO_2 nanomaterial toward a model compound, i.e., octachloronaphthalene (CN-75), which is fully substituted with chlorine atoms, was evaluated at 300 °C. The degradation products, especially the oxidation products, were comprehensively investigated using gas chromatography–mass spectrometry (GC/MS) combined with silicane derivatization, high-performance liquid chromatography/hybrid quadrupole time-of-flight mass spectrometry (HPLC/Q-TOF-MS/MS), and ion chromatography (IC). Electron spin resonance (ESR) experiments, in combination with X-ray photoelectron spectroscopy (XPS) analysis of the TiO_2, were used to study the role of reactive oxygen species in the degradation of CN-75. An oxidative degradation mechanism was proposed based on the findings. The results will be useful in developing methods for eliminating PCN-concentrated wastes.

Results

Kinetic study. The time-dependent degradation behavior of CN-75 (990.1 nmol) over anatase TiO_2 at 300 °C was investigated. The black squares in Fig. 1 represent changes in the amount of residual CN-75 with heating time at 300 °C, calculated based on quasi-exponential decay. The amount of CN-75 decreased from 990.1 to 78.28 nmol in 60 min. This suggests that nanosized anatase TiO_2 is an effective catalyst

for CN-75 degradation. A linear $\ln(R_{CN\text{-}75}/I_{CN\text{-}75})$ versus time plot corresponding to pseudo-first-order reaction kinetics with an initial rate constant k_{obs} (min^{-1}) of 0.04 was obtained as shown in the inset in Fig. 1($I_{CN\text{-}75}$ is the initial number of moles of CN-75, and $R_{CN\text{-}75}$ is the number of moles of the remained CN-75 following heating for a given time period). It can be seen from Fig. 1 that only a small amount of 1,2,3,4,5,6,7-heptachloronaphthalene (CN-73) was detected in the hydrodechlorination products from 5 to 60 min. In contrast, in the progress of CN-75 degradation over as-prepared Fe_3O_4 with the similar dosage for the same reaction phases, a series of hydrodechlorination products from heptachloronaphthalenes to dichloronaphthalenes were detected[19]. The hydrodechlorination reaction of CN-75 was less favored on anatase TiO_2 than on Fe_3O_4. This may be because the stability of anatase TiO_2 is higher than that of Fe_3O_4, as shown by the higher EBG of anatase TiO_2 (3.2 eV) compared with that of Fe_3O_4 (0.1 eV). Similarly, the weaker hydrodechlorination of decachlorobiphenyl was also found in its degradation over $NiFe_2O_4$ with EBG at 2.19 eV than over Fe_3O_4[20].

GC/MS analysis of oxidation products after derivatization. Competition between hydrodechlorination and oxidation reactions in the degradation of chlorinated benzenes over metal oxides has often been reported[9,12,20,21]. The reason is that lower chlorinated products and oxidation products, such as phenolate, acetate, and carbon monoxide species, have been detected simultaneously[9,22,23]. This may be explained by different types of active centers on catalysts. One of the reactions will be the main process, depending on the reaction conditions and reactants. A low level of hydrodechlorination suggests that oxidative degradation occurs preferentially. The oxidation intermediate products formed during catalytic degradation of CN-75 were studied to obtain a better understanding of the degradation pathway. Theurich *et al.*[24] reported that 15 different oxidation intermediates were identified during the photocatalytic degradation of naphthalene in aqueous suspensions of TiO_2 under UV irradiation. To evaluate the existence of oxidative intermediates during the reaction, the dosage of CN-75 increased from 990.1 nmol to 4,950.5 nmol. GC/MS is often used to identify unknown substances. However, the response of the oxidative degradation products often with high polarity was poor in GC/MS. Silylation is one of the derivatization procedures widely used to improve GC behavior of polar compounds containing phenolic and carboxylic groups. In this procedure, the active hydrogens could be replaced by trimethylsilyl groups, producing derivatives which are more volatile and thermally stable. Albero *et al.*[25] reported that phenolic and carboxylic compounds in soil, such as parabens, bisphenols and triclosan, were determinated by gas chromatography tandem mass spectrometry with *in situ* derivatization of N,O-bis(trimethylsilyl)trifluoroacetamide with 1% trimethylchlorosilane (BSTFA:TMCS = 99:1, v/v). Saitta *et al.*[26] also demonstrated 21 phenolic compounds in Italian and Turkish pistachio oil samples by means of the mass spectra of the BSTFA-TMCS derivatives. In present study, the reaction products were derivatized using BSTFA:TMCS (99:1)[27], and then analyzed using GC/MS in EI full-scan mode. The main derivatization reactions are as follows:

$$\text{R–OH} + \text{BSTFA} \rightarrow \text{R–O–Si}(\text{CH}_3)_3 \quad (1)$$

$$\text{R–COOH} + \text{BSTFA} \rightarrow \text{R–COO–Si}(\text{CH}_3)_3 \quad (2)$$

Figure 2 shows the GC/MS chromatograms of the chemically derivatized samples after CN-75 degradation over anatase TiO_2 at 300 °C for 5 min. Analysis of the derivatized products showed that tetrachlorophenol, tetrachlorobenzoic acid, tetrachloroacroleinbenzoic acid, tetrachlorophthalaldehyde, tetrachlorosalicylic acid, and hexachloronaphthols were produced. The list of corresponding oxidation products is given in Table 1. Full-scan MS analysis was performed to identify the structures of the detected oxidation derivatives. Qualitative analysis was performed based on the molecular ions, fragment ions, the ratio between ^{35}Cl and ^{37}Cl, and comparison with data in the NIST02 standard spectral database[28]. As shown in Fig. 2, clear molecular ions and fragment ions were observed for seven derivatized products. For example, the mass spectrum corresponding to Peak P2 showed the presence of derivatized tetrachlorobenzoic acid. A clear molecular ion $[M]^+$ at *m/z* 332, and fragmentation clusters at *m/z* 317 $[M-CH_3]^+$, 243 $[M-OSi(CH_3)_3]^+$, 215 $[M-COOSi(CH_3)_3]^+$, 178 $[M-ClCOOSi(CH_3)_3]^+$, and 143 $[M-2ClCOOSi(CH_3)_3]^+$were observed. The isotope distributions fit a four Cl atom profile (the ratio of the peaks at *m/z* 332 and 334 was 1:1.3). This information clearly identifies the product as tetrachlorobenzoic acid[29]. The mass spectrum corresponding to Peak P4 showed the presence of tetrachlorophthalaldehyde[30]. The mass spectrum showed a molecular ion $[M]^+$ at *m/z* 272 and a fragmentation cluster at *m/z* 243 $[M-CHO]^+$. The mass spectrum of Peak P7, corresponding to the derivative of hexachloronaphthol, showed a molecular ion $[M]^+$ at *m/z* 422 and typical fragmentation clusters at *m/z* 407 $[M-CH_3]^+$ and 372 $[M-ClCH_3]^+$. The identification of naphthalene rings and single benzene rings with –OH, –COOH, and –CHO substituents confirmed that oxidation reactions occurred. The presence of oxidation intermediates containing single benzene rings indicated partial splitting of the naphthalene rings during the oxidative degradation reaction. In contrast, the oxidative products only with naphthalene-ring, i.e., tetrachloronaphthols and dihydrodiol, have been determined by GC-MS during the biodegradation of 1,4-dichloronaphthalene[31].

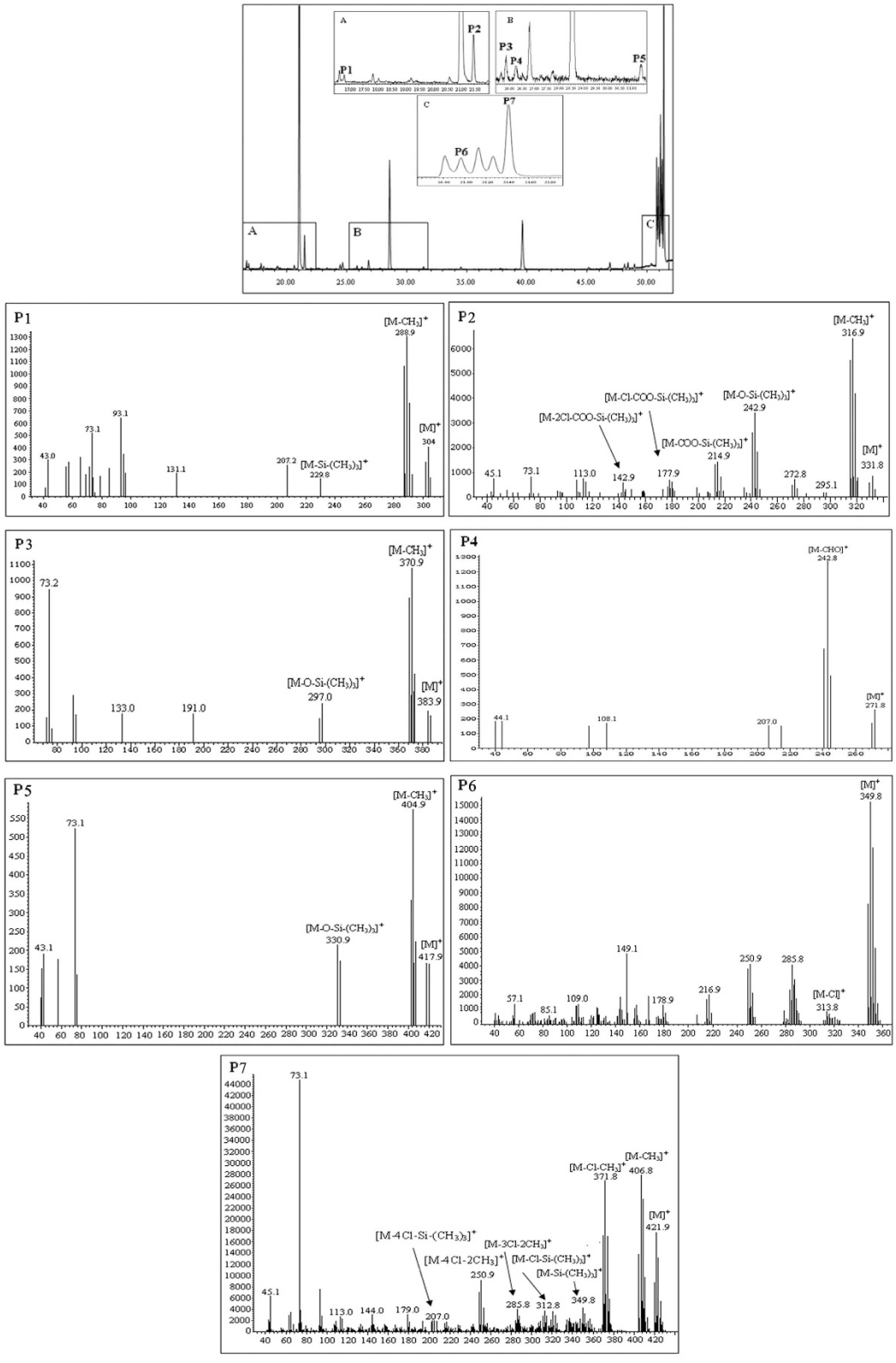

Figure 2. GC/MS chromatograms of derivatized products of CN-75 degradation over anatase TiO_2 at 300 °C for 5 min.

HPLC/Q-TOF-MS/MS analysis of oxidation products. LC/MS is a sensitive analytical technique that is widely used for the separation and quantification of highly polar products[32,33]. During the analytical process, polar oxidation products are efficiently ionized using the ionization techniques associated with LC/MS, enabling their identification[34]. This technique has been often applied together with GC/MS

Peak number	Retention time	Derivative structure	Product structure	Product name
P1	16.83	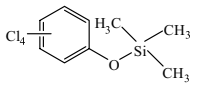	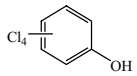	Tetrachloro-phenol
P2	21.49	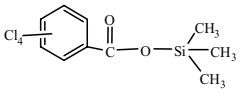	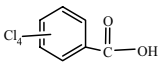	Tetrachloro-benzoic acid
P3	25.85	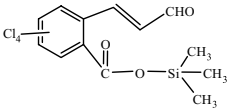	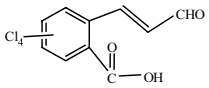	Tetrachloro-acrolein-benzoic acid
P4	26.27	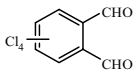	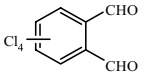	Tetrachloro-phthalaldehyde
P5	31.39	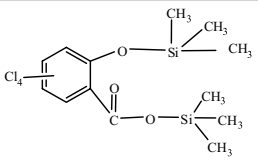	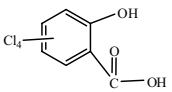	Tetrachloro-salicylic acid
P6	50.96	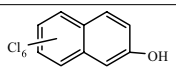	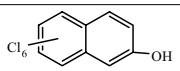	Hexachloro-naphthol
P7	51.41	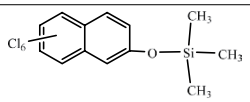	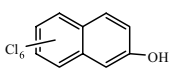	Hexachloro-naphthol

Table 1. Oxidative products following degradation of CN-75 over anatase TiO_2 at 300 °C for 5 min, determined by GC/MS after the derivatization.

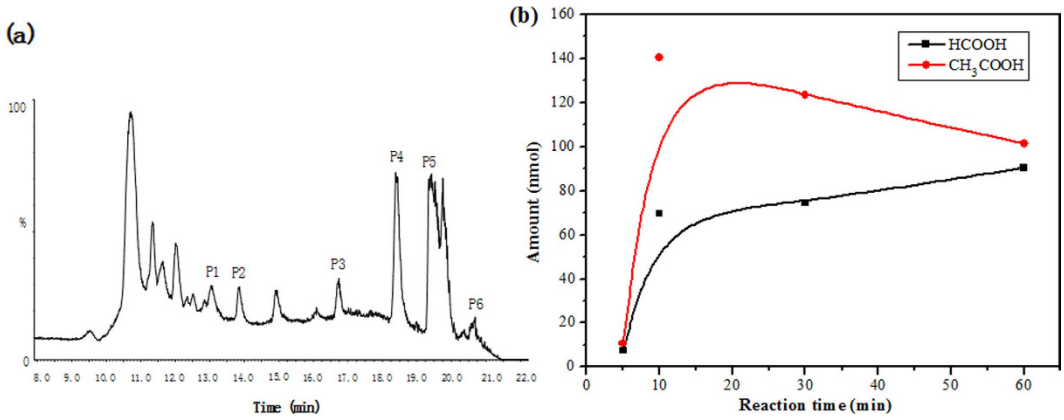

Figure 3. (**a**) HPLC spectrum of chemical species obtained by degradation of CN-75 over anatase TiO_2 at 300 °C for 5 min and (**b**) distribution profiles of organic acids formed during degradation of CN-75 over anatase TiO_2 at 300 °C.

to comprehensively determine the polar species[35]. The oxidation process was therefore further investigated by monitoring the formation of oxidation intermediate products during the catalytic degradation of CN-75 over anatase TiO_2 using HPLC/Q-TOF-MS/MS. Figure 3a shows the HPLC results for the chemical species following reaction between CN-75 (4,950.5 nmol) and anatase TiO_2 (50 mg) at 300 °C for 5 min. Tetra-chlorophenols, tetrachlorobenzenedihydrodiol, hydroxypentachloronaphthalenedione (OH-PeCN-dione), hydroxypentachloronaphthalene (OH-PeCN), and hydroxyhexachloronaphthalene (OH-HxCN) were determined as degradation products (Table 2). However, the isomer patterns of the hydroxyl congeners could not be identified because of limitations associated with the external standards.

Peak number	Retention time (min)	Qualitative ions	Compound name	Chemical structure
P1	13.1	213, 215, 217	Tetrachlorobenzene- dihydrodiol	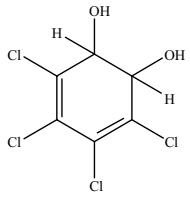
P2	13.9	229, 231, 233	Tetrachlorophenol	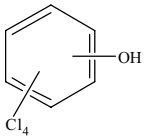
P3	16.7	342, 344, 346	hydroxyl–pentachloronaphthalene–dione	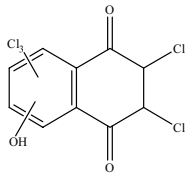
P4	18.5, 19.8	313, 315, 317	hydroxyl-pentachloronaphthalene	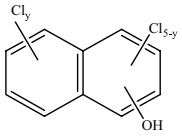
P5, P6	19.5, 20.7	347, 349, 351	hydroxyl-hexachloronaphthalene	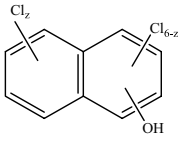

Table 2. Oxidative products following degradation of CN-75 over anatase TiO_2 at 300 °C for 5 min, determined by HPLC/Q-TOF-MS/MS.

These results further show that oxidation intermediates with naphthalene rings and single benzene rings were produced during the oxidative degradation reaction. However, the only hydroxyl-oxidative products with naphthalene ring, i.e. hydroxyl-trichloronaphthalene (TrCN), -tetrachloronaphthalene (TeCN), -PeCN, and -HxCN have been determined by HPLC/Q-TOF-MS/MS during the degradation of CN-75 on Fe_3O_4[19]. This suggests the occurrence of deep oxidative degradation of CN-75 on anatase-type TiO_2.

Analysis of oxidation products by IC. Literature reports have indicated that chlorinated aromatic compounds containing hydroxyl, aldehyde, and carboxyl groups can be easily ring-cracked to smaller organic molecules such as formate and acetate[11]. Ma *et al.*[36] detected the formation of surface formate species using *in situ* FTIR spectroscopy in low-temperature 1,2-dichlorobenzene oxidation over water-resistant Fe–Ca–O_x/TiO_2 catalysts. Similar results were reported for the catalytic oxidation of 1,2-dichlorobenzene over Ca-doped FeO_x hollow microspheres[37]. Formic, acetic, and propanoic acids have been detected during degradation of decachlorobiphenyl over Fe_3O_4[19]. In the current study, ring-cracked products were detected, using IC, in the reaction between CN-75 (990.1 nmol) and anatase TiO_2 (50 mg) at 300 °C. Formic and acetic acids were the main ring-cracked degradation products, as shown in Fig. 3b. The amount of acetic acid rapidly increased to a maximum of 140.6 nmol after heating for about 10 min, and then decreased with heating time. In contrast, the formic acid content increased steadily with heating time, with a maximum content of 90.4 nmol at 60 min. These oxidation products indicate that TiO_2 also facilitates the ring-cracking oxidation pathway of chlorinated aromatics.

Discussion

The presence of active oxygen species on nanosized anatase TiO_2 catalysts is believed to contribute to the occurrence of oxidation reactions during CN-75 degradation[19]. The O 1s XP spectrum of the anatase TiO_2 catalyst is shown in Fig. 4a. The peak at 530.97 eV (denoted by P1) is attributed to surface oxygen and adsorbed oxygen species, and the peak located at 529.15 eV (denoted by P2) is attributed to lattice oxygen[38]. Similar oxygen species were detected on the surface of Ca-doped FeO_x hollow microspheres and $CaCO_3$/α-Fe_2O_3 composite catalysts[37]. A high proportion of surface oxygen on the metal oxide catalyst increases the activity in low-temperature oxidative degradation of 1,2-dichlorobenzene.

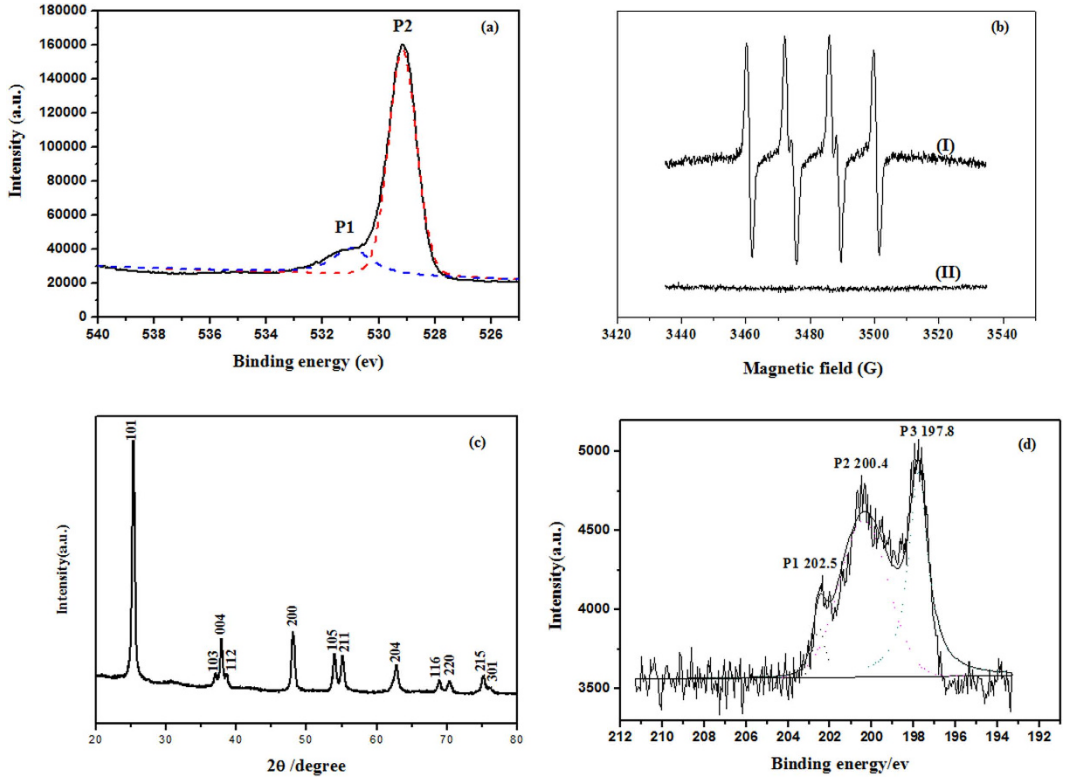

Figure 4. (**a**) O 1s XPS spectrum of TiO_2 catalyst, (**b**) ESR spectra of $O_2^{-\bullet}$ (I) and •OH (II) generated by reaction of anatase TiO_2 and CN-75 at 300 °C for 10 min, (**c**) XRD pattern of TiO_2 catalyst and (**d**) Cl 2p XPS spectrum of TiO_2 sample after the reaction for 10 min.

Reactive oxygen species such as $O_2^{-\bullet}$ and •OH are strong electrophilic oxidants. They can attack organic substrates, leading to their degradation and ultimately to their total mineralization to CO_2 and H_2O[39,40]. Its role in a range of photocatalytic oxidative degradation reactions, including those of pathogenic bacteria over $NiO/SrBi_2O_4$[41], rhodamine B over TiO_2[42], and azo dyes over Ag/AgBr/TiO[43], have been confirmed by ESR spectroscopy. ESR spectroscopy, with DMPO as the spin-trapping agent, was used to obtain information on the active radicals involved, to determine whether $O_2^{-\bullet}$ and •OH were available products in the decomposition of CN-75 over anatase TiO_2. A reaction was performed between anatase TiO_2 (50 mg) and CN-75 (990.1 nmol) at 300 °C for 10 min. The reaction products were immediately dissolved in dimethyl sulfoxide (DMSO), and then characterized using an ESR analyzer, as shown in Fig. 4b. Four peaks were observed, and the hyperfine constants, i.e., $\alpha_N = 12.7429$ G, $\alpha_H = 10.0304$ G, and $g = 2.0103$, coincided with those previously reported for DMPO–$O_2^{-\bullet}$ (Fig. 4b-I)[9]. The results identify that the superoxide anion may be involved in CN-75 degradation, resulting in the formation of a series of oxidation products and perhaps even into formic acid and acetic acid. The DMPO–·OH species were examined under identical conditions, except water was used as the solvent instead of DMSO. No obvious signal was observed, as shown in Fig. 4b-II. This differs from the photocatalytic degradation of many organic molecules, in which ·OH species are often identified[41–43].

An oxidative degradation pathway (Fig. 5) is proposed, based on the available oxygen species and the detected oxidation intermediates. The (101) surface is the most stable and frequent surface of anatase TiO_2, as shown in Fig. 4c, which was therefore selectively took as a model[44–46]. It has the same periodicity as the bulk truncated surface and exposes undercoordinated pentacoordinated Ti cations (Ti_{5c}) and dicoordinated oxygen anions (O_{2c}), and fully coordinated Ti_{6c} cations and tricoordinated oxygen anions (O_{3c})[47]. Coordination theory states that unsaturated ions are prone to bond with ligands[23]. It is therefore hypothesized that CN-75 molecules are adsorbed on the anatase TiO_2 surface via coordination interactions between Lewis acid Ti_{5c} cations and Lewis base Cl[21]. When CN-75 degraded on the surface of the anatase TiO_2 catalyst, firstly, dissociative adsorption of CN-75 on the central Ti_{5c} cations occurs, followed by the attack of carbon atom potential to accepting the electrons by reactive nucleophilic oxygen O^{2-} species. This results in C–Cl bond cleavage and subsequent Ti–Cl bond formation. Association of the free chloride ions with Lewis acid Ti ions occurs during CN-75 degradation over anatase TiO_2. This is confirmed by the Cl 2p core-level XP spectrum of the catalyst after heating for 10 min (Fig. 4d). Three peaks (denoted by P1, P2, and P3) are observed. The peak at 197.8 eV corresponds to Cl bonded to Ti^{4+}, with a net charge of −1, indicating possible formation of $TiCl_4$ during degradation of CN-75[48]. In this

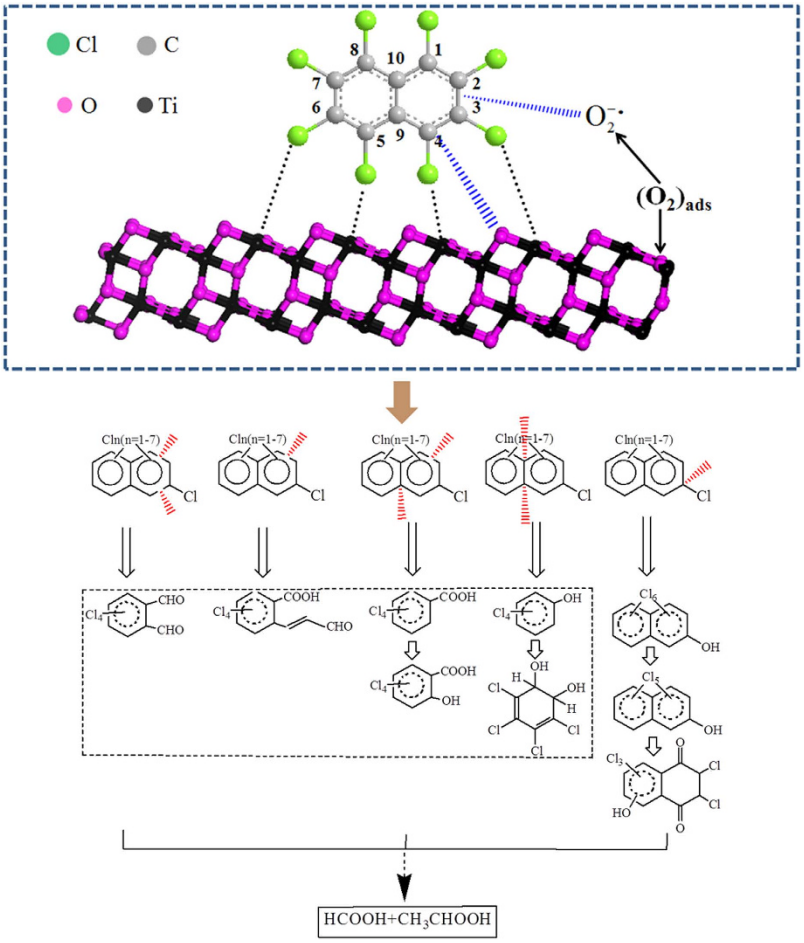

Figure 5. Possible degradation pathways of CN-75 over anatase TiO_2.

reaction pathway, OH-HxCN and OH-PeCN can be formed via nucleophilic attack by basic O^{2-}. Further nucleophilic attack can occur at other positions on PCNs, forming species such as OH-PeCN-dione. The formation of naphthol species was detected during photocatalytic degradation of naphthalene over TiO_2[24].

Superoxide $O_2^{-\bullet}$ species are electrophilic. They have been reported to be formed by transformation of adsorbed O_2 molecules[19,49]. When a subsurface oxygen vacancy is present, it is energetically favorable for O_2 to adsorb at a Ti_{5c} site close to this defect. On adsorption, the extra charge associated with the defect is transferred to the O_2 molecule, converting it to a superoxide $O_2^{-\bullet}$ species. The strongly reactive electrophilic $O_2^{-\bullet}$ species can attack the π-electron cloud of the naphthalene ring, which has a highly dense electron population. This leads to the cracking of the naphthalene ring at different positions. The detection of tetrachlorophenol and the resultant tetrachlorobenzenedihydrodiol indicates that one of the rings in the naphthalene ring of CN-75 is first opened through C_1–C_{10} and C_4–C_9 bond cleavage. Breakage of the C_1–C_2 and C_4–C_9 bonds in one ring could result in the formation of tetrachlorobenzoic acid, which is further oxidized to tetrachlorosalicylic acid. Similarly, the breakage of C_1–C_2 or and C_3–C_4 bonds could lead to the formation of tetrachloroacroleinbenzoic acid or and tetrachlorophthalaldehyde, respectively. These results show that lateral cleavage of one naphthalene ring at different C–C bond positions by electrophilic $O_2^{-\bullet}$ could occur, leading to formation of various single-benzene-ring oxidation products. Unexpectedly, the symmetric half section of CN-75 could be retained along with generation of complex oxidation products containing the tetrachlorobenzene structure.

It is important to note that the reaction pathways via electrophilic and nucleophilic attack by reactive oxygen species such as O^{2-} and $O_2^{-\bullet}$ are not independent of each other. The newly formed chlorinated naphthol species can also be attacked by reactive oxygen species such as $O_2^{-\bullet}$. Moreover, oxidation products with both naphthalene and single benzene rings can be further attacked by reactive oxygen species, and completely cracked to small molecules such as formic and acetic acids. A wide range of oxidation products such as naphthols, phenols, hydroxy-diones, benzoic acids, acroleinbenzoic acid, phthalaldehyde, salicylic acid, dihydrodiols, and formic and acetic acids, with chlorinated naphthalene or benzene rings, or without aromatic rings, were detected during the degradation of CN-75 over anatase TiO_2. This

is different from the previously reported results for CN-75 degradation over Fe_3O_4 micro/nanomaterials[19], in which only chloronaphthol species, and formic acid and acetic acids were detected as the oxidation products under the same experimental conditions. This shows that oxidative degradation of CN-75 on anatase TiO_2 was more extensive that on Fe_3O_4 micro/nanomaterials. Deep oxidative degradation of CN-75 on anatase TiO_2 occurs possibly because of the electronic structure with an EBG of 3.2 eV and the reactive oxygen species on its surface.

Methods

Chemical reagents. Anatase TiO_2 (nanopowder, diameter <25 nm) was supplied by Sigma-Aldrich (USA). CN-75 (Supelco, USA) was laboratory analytical grade and used without further purification. HPLC-grade ethyl acetate was purchased from Fisher Scientific (Geel, Belgium). Chromatographic-grade methanol, acetonitrile, and hexane were purchased from Dika Technologies (Lake Forest, CA, USA). Derivatization reagents, BSTFA:TMCS = 99:1 were supplied by Supelco (USA).

Degradation experiments. Degradation experiments were performed in sealed glass ampoules. Prior to the reaction, a hexane solution of CN-75 (990.1 or 4,950.5 nmol) was injected into an ampoule and subsequently evaporated to dryness at room temperature, and then mixed with later added 50 mg of anatase TiO_2. The samples were heated at 300 °C for an appropriate time. A blank experiment was performed in the absence of TiO_2 under the same conditions. All experiments were performed in triplicate to ensure repeatability of the results.

Degradation product analysis. After the decomposition reaction, the ampoule was cooled to room temperature and crushed, and the sample was extracted. The unreacted CN-75 and newly formed PCNs were analyzed using an Agilent 6890 gas chromatograph equipped with a DB-5 MS capillary column (30 m × 0.25 mm i.d., 0.25 μm film thickness) and an Agilent 5973 N mass selective detector. Helium ($\geq$99.999%) at a flow rate of 1 mL/min was used as the carrier gas, and the injector was set at 260 °C. The column temperature was set at 75 °C for 2 min, gradually increased to 150 °C at 20 °C/min, then increased to 205 °C at 1.5 °C/min, and finally increased to 270 °C at 2.5 °C/min. The diluted sample (1.0 μL) was injected in split-less mode. An electron ionization system with an ionization energy of 70 eV was used.

For oxidation product analysis, the reaction products obtained after CN-75 degradation over anatase TiO_2 at 300 °C for 5 min were extracted by the mixture solvent of hexane/ methanol/ ethyl acetate (1:1:1, v/v/v). The extract was dehydrated using a column packed with anhydrous sodium sulfate, and then evaporated under stream of nitrogen to dryness. Dry residue was dissolved in 0.2 mL of derivatizing reagent BSTFA:TMCS (99:1) and vortexed. The mixture reacted at room temperature for 60 min, and the derivatization products were analyzed using GC/MS. The column temperature was initially 50 °C, and increased to 180 °C (for 2 min) at 10 °C/min, to 210 °C at 1 °C/min, and to 280 °C at 10 °C/min. The carrier gas was helium at a flow rate of 1 mL/min.

The oxidation products were also analyzed using HPLC/Q-TOF-MS/MS (Micromass Q-TOF micro, Waters, USA). After the degradation of CN-75 (4,950.5 nmol) over anatase TiO_2, product samples were extracted using HPLC-grade methanol, filtered through a 0.45 μm mesh membrane, and concentrated to approximately 100 μL. The oxidation products were detected using a Supelcosiltmlc-18 C18 column (Sigma; 4.6 mm × 250 mm; 5 μm particle size). The elution flow rate was 0.5 mL/min with a gradient of 0.1% acetic acid in water–acetonitrile [acetonitrile concentrations 0% (isocratic, 5 min), 70% (isocratic, 5 min), 70–90% (linear, 5 min), 90–100% (linear, 5 min), 100% (isocratic, 5 min), and 0% (isocratic, 4 min)]. MS was performed using a Waters Micromass Quattro Premier XE (triple-quadrupole) detector, equipped with an electrospray ionization (EI) source (Micromass, USA). The mass analyzer was operated in negative ionization (EI^-) mode and the optimized parameters were source temperature 120 °C, desolvation temperature 200 °C, capillary voltage 2.50 kV, desolvation gas flow rate 600 L/h, and cone gas flow rate 50 L/h.

The organic acid oxidation products such as acetic and formic acid were analyzed using IC. The degradation samples obtained from the reaction of CN-75 (990.1 nmol) and anatase TiO_2 (50 mg) were extracted three times with 15 ml deionized water for 10 min each time under ultrasonication. And then the combined extracts were filtered through a 0.45 μm mesh membrane for IC measurements. The employed IC was a DIONEX AS 5000 instrument equipped with an AS-AP automated sampler. A Dionex AS11-HC guard column (50 × 4 mm i.d.) and a Dionex AS11-HC analytical column (250 × 4 mm i.d.) were used for the analyses. The analyses were performed at 30 °C with a potassium hydroxide eluent that was generated from a Dionex EG on line and run with a linear gradient at a flow rate of 1.0 mL min^{-1}.

XPS and ESR. The surface element oxidation states of the TiO_2 catalyst, which reacted with CN-75 at 300 °C for 10 min, were investigated using XPS (Escalab 250), with monochromated Al Kα (1,486.6 eV) radiation (200 W, 200 eV) as the X-ray source. The operating pressure was ~1×10^{-8} Torr.

The radical species formed during degradation were investigated using ESR spectroscopy (ESP 300 E electron paramagnetic resonance spectrometer, Bruker) with 5,5-dimethyl-1-pyrroline *N*-oxide (DMPO; Sigma Chemical Co.) as the spin-trapping agent. Typically, anatase TiO_2 (50 mg) and CN-75 (990.1 nmol) reacted at 300 °C for 10 min. A reaction using anatase TiO_2 but without CN-75 was also examined under

the same conditions for comparison. The settings for the ESR spectrometer were center field, 3,485 G; sweep width, 100.0 G; microwave frequency, 9.8 GHz; and power, 10 mW.

References

1. *Seventh meeting of the Conference of the Parties to the Stockholm Convention*. (2015) Available at: http://synergies.pops.int/2015COPs/MeetingDocuments/tabid/4243/language/en-US/Default.aspx. (Accessed: 4th July 2015).
2. Haglund, P. Determination of polychlorinated naphthalenes in polychlorinated biphenyl products via capillary gas chromatography-mass spectrometry after separation by gel permeation chromatography. *J. Chromatogr.* **634,** 79–86 (1993).
3. *Seventh meeting of the Persistent Organic Pollutants Review Committee (POPRC7).* (2011) Available at: http://chm.pops.int/Convention/POPsReview Committee/POPRCMeetings/POPRC7/POPRC7Documents/tabid/2267/language/en-US/Default.aspx. (Accessed: 5th July 2015).
4. Yamashita, N., Kannan, K., Imagawa, T., Miyazaki, A. & Giesy, J. P. Concentrations and Profiles of Polychlorinated Naphthalene Congeners in Eighteen Technical Polychlorinated Biphenyl Preparations. *Environ. Sci. Technol.* **34,** 4236–4241 (2000).
5. Abad, E., Caixach, J. & Rivera, J. Dioxin like compounds from municipal waste incinerator emission: assessment of the presence of polychlorinated naphthalenes. *Chemosphere* **38,** 109–120 (1999).
6. Imagawa, T. & Lee, C. W. Correlation of polychlorinated naphthalenes with polychlorinated dibenzofurans formed from waste incineration. *Chemosphere* **44,** 1511–1520 (2001).
7. Crookes, M. J. & Howe, P. D. Environmental hazard assessment: Ethyl benzene. In: Toxic Substances Division, Directorate for Air, Climate and Toxic Substances. *Department of the Environment, Watford, U.K.* (1993).
8. *Ninth meeting of the Persistent Organic Pollutants Review Committee (POPRC9).* (2013) Available at: http://chm.pops.int/TheConvention/POPsReviewCommittee/Meetings/POPRC9/Documents/tabid/3281/Default.aspx. (Accessed: 1th July 2015).
9. Lin, S. J. *et al.* The degradation of 1,2,4-trichlorobenzene using synthesized Co_3O_4 and the hypothesized mechanism. *J. Hazard. Mater.* **192,** 1697–1704 (2011).
10. Jia, M. K., Su, G. J., Zheng, M. H., Zhang, B. & Lin, S. J. Development of self-assembled 3D Fe_xO_y micro/nano materials for application in hexachlorobenzene degradation. *J. Nanosci. Nanotechnol.* **11,** 2100–2106 (2011).
11. Krishnamoorthy, S., Rivas, J. A. & Amiridis, M. D. Catalytic oxidation of 1,2-dichlorobenzene over supported transition metal oxides. *J. Catal.* **193,** 264–272 (2000).
12. Lichtenberger, J. & Amiridis, M. D. Catalytic oxidation of chlorinated benzenes over V_2O_5/TiO_2 catalysts. *J. Catal.* **223,** 296–308 (2004).
13. Wang, J. *et al.* Catalytic oxidation of chlorinated benzenes over V_2O_5/TiO_2 catalysts: The effects of chlorine substituents. *Catal. Today* **241,** 92–99 (2015).
14. Weber, R. & Sakurai, T. Low temperature decomposition of PCB by TiO_2-based V_2O_5/WO_3 catalyst: evaluation of the relevance of PCDF formation and insights into the first step of oxidative destruction of chlorinated aromatics. *Appl. Catal. B* **34,** 113–127 (2001).
15. Gannoun, C. *et al.* Elaboration and characterization of sulfated and unsulfated V_2O_5/TiO_2 nanotubes catalysts for chlorobenzene total oxidation. *Appl. Catal. B* **147,** 58–64 (2014).
16. Fujishima, A. & Kudo, K. Electrochemical photolysis of water at a semiconductor electrode. *Nature* **238,** 37–38 (1972).
17. Linsebigler, A. L., Lu, G. Q. & Jr, J. T. Y. Photocatalysis on TiO_2 Surfaces: principles, mechanisms, and selected results. *Chem. Rev.* **95,** 735–758 (1995).
18. Obata, K. *et al.* Photocatalytic decomposition of NH_3 over TiO_2 catalysts doped with Fe. *Appl.Catal. B* **160-161,** 200–203 (2014).
19. Su, G. J. *et al.* Thermal degradation of octachloronaphthalene over as-prepared Fe_3O_4 micro/nanomaterial and its hypothesized mechanism. *Environ. Sci. Technol.* **48,** 6899–6908 (2014).
20. Huang, L. Y. *et al.* Degradation of polychlorinated biphenyls using mesoporous iron-based spinels. *J. Hazard. Mater.* **261,** 451–462 (2013).
21. Zhang, L. F., Zheng, M. H., Liu, W. B., Zhang, B. & Su, G. J. A method for decomposition of hexachlorobenzene by γ-alumina. *J. Hazard. Mater.* **150,** 831–834 (2008).
22. Ma, X. D., Sun, H. W., He, H. & Zheng, M. H. Competitive reaction during decomposition of hexachlorobenzene over ultrafine Ca–Fe composite oxide catalyst. *Catal. Lett.* **119,** 142–147 (2007).
23. Ma, X. D. *et al.* Synergic effect of calcium oxide and iron (III) oxide on the dechlorination of hexachlorobenzene. *Chemosphere* **60,** 796–801 (2005).
24. Theurich, J. & Bahnemann, D. W. Photocatalytic degradation of naphthalene and anthracene: GC-MS analysis of the degradation pathway. *Res. Chem. lntermed.* **23,** 247–274 (1997).
25. Albero, B., Sánchez-Brunete, C., Miguel, E., Pérez, R. A. & Tadeo, J. L. Determination of selected organic contaminants in soil by pressurized liquid extraction and gas chromatography tandem mass spectrometry with *in situ* derivatization. *J. Chromatogr. A* **1248,** 9–17 (2012).
26. Saitta, M., La Torre, G. L., Potortì, A. G., Di Bella, G. & Dugo, G. Polyphenols of pistachio (pistacia vera L.) oil samples and geographical differentiation by principal component analysis. *J. Am. Oil Chem. Soc.* **91,** 1595–1603 (2014).
27. Wenclawiak, B. W., Jensen, T. E. & Richert, J. F. O. GC/MS-FID analysis of BSTFA derivatized polar components of diesel particulate matter (NBS SRM-1650) extract. *Fresenius J. Anal. Chem.* **346,** 808–812 (1993).
28. Su, G. J. *et al.* Synergetic effect of alkaline earth metal oxides and iron oxides on the degradation of hexachlorobenzene and its degradation pathway. *Chemosphere* **90,** 103–111 (2013).
29. Wasada, N. *Spectral Database for Organic Compounds SDBS*. (2015) Available at: http://sdbs.db.aist.go.jp/sdbs/cgi-bin/direct_frame_disp.cgi?sdbsno=51814. (Accessed: 25th Aprel 2015).
30. Oh, J. A. & Shin, H. S. Determination of ortho-phthalaldehyde in water by high performance liquid chromatography and gas chromatography-mass spectrometry after hydrazine derivatization. *J. Chromatogr. A* **1247,** 99–103 (2012).
31. Mori, T., Nakamura, K. & Kondo, R. Fungal hydroxylation of polychlorinated naphthalenes with chlorine migration by wood rotting fungi. *Chemosphere* **77,** 1230–1235 (2009).
32. Erratico, C. A., Szeitz, A. & Bandiera, S. M. Validation of a novel *in vitro* assay using ultra performance liquid chromatography-mass spectrometry (UPLC/MS) to detect and quantify hydroxylated metabolites of BDE-99 in rat liver microsomes. *J. Chromatogr. B* **878,** 1562–1568 (2010).
33. Mas, S. *et al.* Comprehensive liquid chromatography-ion-spray tandem mass spectrometry method for the identification and quantification of eight hydroxylated brominated diphenyl ethers in environmental matrices. *J. Mass Spectrom.* **42,** 890–899 (2007).
34. Sun, J. T. *et al.* Sample preparation method for the speciation of polybrominated diphenyl ethers and their methoxylated and hydroxylated analogues in diverse environmental matrices. *Talanta* **88,** 669–676 (2012).
35. Bian, W. J., Song, X. H., Liu, D. Q., Zhang, J. & Chen, X. H. The intermediate products in the degradation of 4-chlorophenol by pulsed high voltage discharge in water. *J. Hazard. Mater.* **192,** 1330–1339 (2011).

36. Ma, X. D. *et al.* Water-resistant Fe–Ca–O_x/TiO_2 catalysts for low temperature 1,2-dichlorobenzene oxidation. *Appl. Catal. A* **466,** 68–76 (2013).
37. Ma, X. D. *et al.* Catalytic oxidation of 1,2-dichlorobenzene over Ca-doped FeO_x hollow microspheres. *Appl. Catal. B* **147,** 666–676 (2014).
38. Wang, X. Y., Kang, Q. & Li, D. Catalytic combustion of chlorobenzene over MnO_x–CeO_2 mixed oxide catalysts. *Appl. Catal. B* **86,** 166–175 (2009).
39. Lai, T. L., Lai, Y. L., Lee, C. C., Shu, Y. Y. & Wang, C. B. Microwave-assisted rapid fabrication of Co_3O_4 nanorods and application to the degradation of phenol. *Catal. Today* **131,** 105–110 (2008).
40. Hoffmann, M. R., Martin, S. T., Choi, W. & Bahnemannt, D. W. Environmental applications of semiconductor photocatalysis. *Chem. Rev.* **95,** 69–96 (1995).
41. Hu, C., Hu, X. X., Guo, J. & Qu, J. H. Efficient destruction of pathogenic bacteria with NiO/$SrBi_2O_4$ under Visible Light Irradiation. *Environ. Sci. Technol.* **40,** 5508–5513 (2006).
42. Zhao, J. C. *et al.* Photoassisted degradation of dye pollutants. 3. degradation of the cationic dye rhodamine B in aqueous anionic surfactant/TiO_2 dispersions under visible light irradiation: evidence for the need of substrate adsorption on TiO_2 particles. *Environ. Sci. Technol.* **32,** 2394–2400 (1998).
43. Hu, C., Lan, Y. Q., Qu, J. H., Hu, X. X. & Wang, A. M. Ag/AgBr/TiO_2 visible light photocatalyst for destruction of azodyes and bacteria. *J. Phys. Chem. B* **110,** 4066–4072 (2006).
44. Liu, L. L. *et al.* O_2 adsorption and dissociation on a hydrogenated anatase (101) Surface. *J. Phys. Chem. C* **118,** 3471–3482 (2014).
45. Aschauer, U. & Selloni, A. Hydrogen interaction with the anatase TiO_2 (101) surface. *Phys. Chem. Chem. Phys.* **14,** 16595–16602 (2012).
46. Islam, M. M., Calatayud, M. & Pacchioni, G. Hydrogen adsorption and diffusion on the anatase TiO_2(101) surface: a first-principles investigation. *J. Phys. Chem. C* **115,** 6809–6814 (2011).
47. Li, Y. F., Aschauer, U., Chen, J. & Selloni, A. Adsorption and reactions of O_2 on anatase TiO_2. *Acc. Chem. Res.* **47,** 3361–3368 (2014).
48. Fleutot, S., Dupin, J. C., Renaudin, G. & Martinez, H. Intercalation and grafting of benzene derivatives into zinc-aluminum and copper-chromium layered double hydroxide hosts: an XPS monitoring study. *Phys. Chem. Chem. Phys.* **13,** 17564–17578 (2011).
49. Li, Y. F. & Selloni, A. Theoretical study of interfacial electron transfer from reduced anatase TiO_2 (101) to adsorbed O_2. *J. Am. Chem. Soc.* **135,** 9195–9199 (2013).

Acknowledgements

This study was supported by the National 973 Program (2015CB453103), the Strategic Priority Research Program of the Chinese Academy of Sciences (XDB14020102), and the National Natural Science Foundation of China (21377147, 21177141, 21321004).

Author Contributions

G.S. and M.Z. conceived and designed the experiments. L.Z., Q. L. and L.Y. conducted the experimental parts. G.S., Q.L. and H.L. analyzed the data and wrote the manuscript. G.S., Q.L., L.H. and M.Z. reviewed the literature and checked the data. All authors have reviewed the manuscript.

Additional Information

Competing financial interests: The authors declare no competing financial interests.

How to cite this article: Su, G. *et al.* Thermal catalytic oxidation of octachloronaphthalene over anatase TiO_2 nanomaterial and its hypothesized mechanism. *Sci. Rep.* **5**, 17800; doi: 10.1038/srep17800 (2015).